

A Novel Power Conversion System for SMES in Pulsed Power Applications

A. Bhardwaj , Senior Member, IEEE, J. Moon , D. N. Nguyen , and S. V. Pamidi , Senior Member, IEEE

(Invited Paper)

Abstract—A novel power conversion system (PCS) topology for superconducting magnetic energy storage (SMES) to deliver the required pulses for large, pulsed loads, such as the pulsed magnets of the user facility at Los Alamos National Laboratory, is reported. The simulation results show that SMES, using the PCS topology, delivers the required pulse shape to the pulsed load and recovers the leftover energy back to SMES. The bidirectional DC/DC converter is an innovative approach to achieve high energy transfer efficiency, precise pulse shaping, and efficient energy recovery. The converter eliminates the traditional H-bridge architecture, introducing a more streamlined and efficient design that excels in energy delivery and recovery. The novel PCS system is scalable and efficient for large power loads such as pulsed magnets.

Index Terms—DC link, energy storage, HTS, power conversion system, pulsed power, SMES, superconducting coils, voltage source converter.

I. INTRODUCTION

SUPERCONDUCTING magnetic energy storage (SMES) is an advanced energy storage technology that offers both high energy and power densities [1]. SMES is particularly attractive for large-scale and high demand pulsed power applications [2]. SMES stores energy in the form of a magnetic field from superconducting magnets with zero electrical resistance, allowing it to be charged and discharged millions of cycles without degradation. SMES is an ideal solution for applications that require rapid energy delivery and precision control with high energy storage and transfer efficiency [3].

SMES has been explored for various domains, including stabilizing power grids, supporting pulsed power systems, and

serving applications such as nuclear fusion and plasma generation [4], [5], [6], [7], [8]. The distinguishing feature of SMES is its instantaneous response time, crucial in maintaining power system stability, especially in environments that experience frequent power fluctuations. Pulsed power loads such as Los Alamos National Laboratory Pulsed Field Facility need high power density to provide the specific required milli-second pulse with specific shapes [9], [10], [11].

One of the primary challenges of SMES technology in maintaining storage efficiency is with the repeated transfer of energy between the storage system and load. This is where the need for efficient Power Conversion Systems (PCS) comes into play. PCS is responsible for handling the charging and discharging cycles of the SMES, ensuring that energy is transferred smoothly and with minimal loss [12], [13], [14], [15], [16]. The PCS must manage the energy flow but also ensure that the power delivered matches the specific requirements of the load. The requirements include precise control over current and voltage, especially important for pulsed power applications [17].

For high-power applications, such as pulsed power systems or pulsed magnets, the PCS must meet additional demands [17], [18]. Pulsed power systems require quick bursts of energy delivered in a highly controlled manner. To achieve controllability, the PCS must be capable of handling rapid switching events and maintaining stability throughout the energy transfer process. Minimizing energy losses during these fast cycles is critical to improving the overall efficiency of the system. Inefficiency in the PCS leads to significant energy losses, which would reduce the overall efficiency and effectiveness of SMES.

This research focuses on a novel PCS design to improve the energy transfer efficiency of SMES in pulsed power applications. The reported system is an improved design over the previously discussed PCS systems [18]. The design is a novel bidirectional DC/DC converter that eliminates the need for H-bridges. Instead, it uses a voltage source converter with one capacitor stage, which charges both directions to regulate the energy transfer and pulse shape. The new design offers a more efficient solution for managing high-energy pulses in SMES powered applications by reducing the number of components and optimizing the control schemes.

Detailed simulations and performance analyses were performed on the PCS for SMES. The results show the PCS design delivers high-energy pulses to the pulsed load and indicate that the bidirectional converter offers efficient and controlled pulsed

Received 2 October 2024; revised 6 March 2025; accepted 7 March 2025. Date of publication 17 April 2025; date of current version 27 May 2025. This work was supported by the NHMFL-PFF, through the NSF under Cooperative Agreement DMR-1644779 and Cooperative Agreement DMR-2128556, in part by the State of Florida, and in part by the Office of Naval Research under Grant N00014-21-1-2124 and Grant N00014-22-1-2640. (Corresponding author: A. Bhardwaj.)

A. Bhardwaj is with the Los Alamos National Laboratory, Los Alamos, NM 87545 USA, and also with the FAMU-FSU College of Engineering and the Center for Advanced Power Systems, Tallahassee, FL 32310 USA (e-mail: ashish@lanl.gov).

J. Moon and S. V. Pamidi are with the FAMU-FSU College of Engineering and the Center for Advanced Power Systems, Tallahassee, FL 32310 USA (e-mail: j.moon@fsu.edu; pamidi@eng.famu.fsu.edu).

D. N. Nguyen is with Los Alamos National Laboratory, Los Alamos, NM 87545 USA (e-mail: doan@lanl.gov).

Color versions of one or more figures in this article are available at <https://doi.org/10.1109/TASC.2025.3561733>.

Digital Object Identifier 10.1109/TASC.2025.3561733

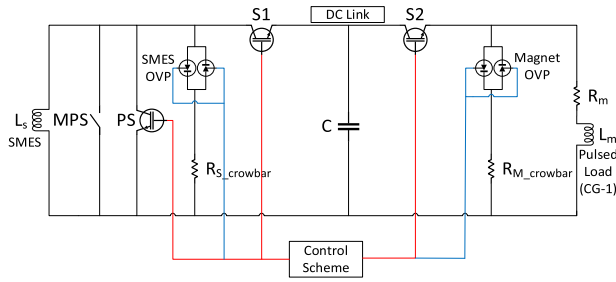


Fig. 2. A schematic of the proposed topology of the novel PCS.

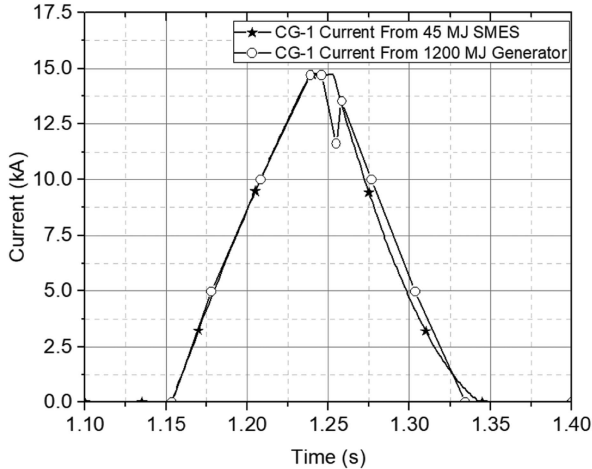


Fig. 1. Operational (generator) and simulated (SMES) current profile comparison of the CG-1 of the 100 T magnet [19] (©[2024] IEEE).

power delivery. These findings provide valuable insights into optimizing PCS for future SMES applications, particularly in national laboratories and other high-demand industrial settings where efficient power delivery is essential.

II. PULSED POWER SYSTEM OVERVIEW

At the National High Magnetic Field Laboratory (NHMFL), SMES systems will play a critical role in powering large-scale pulsed magnets, such as the 100-Tesla magnet [20]. A 1430 MVA motor-generator drives the 100 T magnet. As one of the largest motor-generator setups in the world, it provides the immense energy required to drive the pulsed magnet operations. Coupled with seven 12-pulse thyristor-based power converters, the system ensures smooth and stable power delivery during high-field pulses [21]. The generator, along with PCS, facilitates the controlled transfer of power. The generator's ability to manage rapid, high-power discharges ensures that magnets can reach their peak without instability, enabling the NHMFL's large-scale, user-focused scientific measurements. Fig. 1 compares the current pulses delivered by the 1430 MVA motor-generator with thyristor based 12-pulse converters and a SMES-based H-bridge configuration in the innermost coil group (CG)—1 of the 100 T magnet at NHMFL [19].

One of the critical features of SMES is its ability to enter persistent mode (PM), wherein the current continues to flow and store the energy in the superconducting coil. This capability

allows SMES to achieve rapid response time and minimal energy loss during storage. The total energy stored in a SMES system is determined by the inductance L of the coil and the current I , expressed as: $E = 0.5 LI^2$. SMES can quickly discharge large amounts of energy, making it particularly suitable for pulsed power applications. SMES systems can deliver full power within milliseconds (less than 10 ms). Some of SMES installations have demonstrated the ability to deliver up to 10 MW to 100 MW of power almost instantaneously [22].

III. POWER CONVERSION SYSTEMS FOR SMES

While capable of handling large power, traditional thyristor-based converters often lack the flexibility to control both real and reactive power independently, limiting their application in fast-switching environments [23]. Large H-bridge based converter systems are cost prohibitive. To address these limitations, a novel PCS topology was developed which introduces a bidirectional DC/DC converter that eliminates the need for H-bridges. The design incorporates the use of film capacitors to manage both the charging and discharging phases of the SMES, allowing for more precise pulse shaping and control of energy recovery.

In pulsed power applications, recovering energy from the load and returning it to the storage device is as important as energy delivery itself. Removing the H-bridge reduces the overall system complexity, making the converter more efficient in handling the high-energy pulses required for pulsed power systems. The converter's novel design allows for more efficient bidirectional power flow, improving energy recovery without sacrificing control or performance.

The converter's architecture reported here relies on single DC link capacitors, labeled as C in Fig. 2, to maintain voltage stability across both the SMES and the pulsed load. The IGBT switches in the converter are responsible for controlling the energy flow through the capacitor. During the energy delivery phase, the IGBT switches PS , S_1 , and S_2 along with C are activated to initiate the pulse, manage the energy recovery, and ensure the desired pulse profile in the load. The blue-color lines show the controls of crowbar protection and red-color lines show the controls of PCS operation.

The voltage source converter stage is configured to maintain a steady voltage across the load. This allows the system to generate the flat-top current pulse required for the pulsed power application while delivering the trapezoidal-shaped current pulses to the load. The system handles overvoltage by integrating protection circuits which utilize a crowbar protection scheme to manage overvoltage conditions in both SMES and pulsed load. In the event of a fault, the crowbar system quickly dissipates excess energy, preventing any damage to the system.

The bidirectional converter also supports the efficient return of energy to the SMES from the load. After delivering the desired pulse to the load, any remaining energy after the pulse is recovered and transferred back to the SMES through the link capacitor. This energy recovery process is managed through pulse-width modulation (PWM) techniques, which allow for precise control over the amount of energy returned to the SMES. By efficiently recovering energy, the system can minimize energy losses and

maximize the overall efficiency of the SMES system, a feature important in high-energy systems such as large, pulsed loads.

A. Control Scheme for Bidirectional Converter Topology

The control scheme for the bidirectional DC/DC converter is a critical aspect that ensures the precise operation of the power conversion system. This converter employs a combination of PWM and feedback control loops to regulate the energy transfer between the SMES and the pulsed load. The primary goal of this control scheme is to maintain consistent voltage and current levels during both the charging and discharging phases.

At the core of the control system is an IGBT-based persistent switch (PS) connected across the SMES magnet coil. The switch allows the SMES to remain in persistent mode. The system also includes a slower mechanical or cryogenic superconducting persistent switch (MPS) for maintaining low or zero loss during the waiting time of the pulsed magnets which increases the duration of the energy storage in PM phase.

During the energy transfer stage, the control system initiates the operation by opening the MPS and activating the IGBT-based PS. The energy is then delivered from the SMES to the pulsed load, where the voltage and current levels across the pulsed load are regulated using PWM. By continuously monitoring the voltage across the SMES coil and the pulsed load, the system adjusts the switching behavior of the IGBTs to maintain the desired pulse shape.

Over-voltage protection is an integral part of the control scheme. A crowbar protection circuit is used to safeguard the SMES and the pulsed load in case of a system fault. If the voltage exceeds a predefined threshold, a control signal triggers the thyristor, reducing the output voltage to safe levels. The crowbar ensures that any excess energy is dissipated through a resistive path, protecting the system components from damage. The protection system also handles situations where IGBT switching might fail, providing a fallback to ensure safe operation.

The crowbar is designed to remain engaged until the PS or MPS reconnects the SMES in a persistent mode or the current in the pulsed load reaches zero. This fault-tolerant design adds an additional layer of reliability to the system, ensuring it can safely handle faults without compromising the performance or damaging the pulsed load or SMES.

The energy transfer process is depicted in Fig. 3 by using equivalent circuit models for different operational phases. The models, represented by various switching states of the IGBTs, allow the control system to calculate the ideal conditions for charging, discharging, and freewheeling energy within the system. For example, when charging the capacitor C , the control system opens the MPS, PS and activates IGBT S_1 , routing the energy from the SMES to the capacitor. Once the capacitor reaches its target voltage, the control system switches the SMES in PM. During energy delivery, the control system adjusts the switching of IGBTs PS , S_1 , and S_2 to generate the desired trapezoidal current pulse. As the current reaches the flat-top phase, the system enters a PWM mode, maintaining constant current in the pulsed load. This precise regulation of current and voltage ensures that the system can meet the demand of the pulsed load.

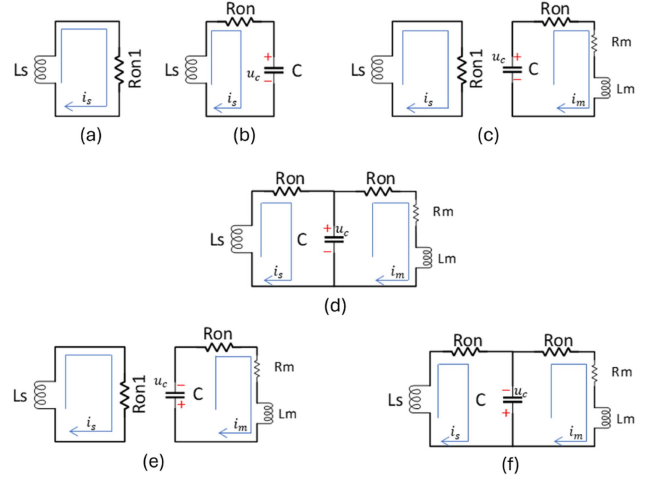


Fig. 3. The circuit schematics of the various operational stages of the novel PCS during the operation of serving the pulsed load.

As the pulse sequence concludes, the system begins the energy recovery phase. Any remaining energy in the pulsed load is transferred back to the SMES via the DC link capacitor C . The control scheme regulates the power delivery, ensuring that the energy is returned efficiently without exceeding the voltage limits of the system.

B. Mathematical Model of the Novel PCS

The mathematical models of the DC/DC converter play a critical role in understanding and optimizing its performance. The operation of the converter is governed by different switching states of the IGBTs and the corresponding equivalent circuits. Each operational phase of the converter, including charging, discharging, and freewheeling, can be described using differential equations that account for the behavior of the SMES coil, capacitors, and pulsed load. Eq. (1) shows the PM phase of the SMES, where $I_{s,0}$ is the initial current in SMES at $t = 0$. The circuit is shown in Fig. 3(a).

$$\begin{aligned} i_s(0) &= I_{s,0} \\ \frac{di_s}{dt} &= -\frac{R_{on1}}{L_s} \cdot i_s \end{aligned} \quad (1)$$

The first operational phase begins with the charging of the capacitor C . In this state, the SMES current i_s is routed through IGBT S_1 , which controls the charging process. The circuit is shown in Fig. 3(b) which happens at time t_1 , and the system's behavior is governed by the following differential equation:

$$\begin{aligned} i_s(t_1) &= I_{s,1} \\ \frac{di_s}{dt} &= -\frac{(u_c + R_{on} \cdot i_s)}{L_s} \\ \frac{du_c}{dt} &= \frac{i_s}{C} \end{aligned} \quad (2)$$

where R_{on1} and R_{on} is the on-state resistance of IGBT PS and S_1 , L_s is the inductance of the SMES coil and u_c is the voltage across the capacitor C . $I_{s,1}$ is the initial current in SMES at $t =$

t_1 . The current i_s represents the flow of energy from the SMES into the capacitor C , which charges to a reference voltage value.

Once the capacitor is charged to the desired level, the system enters the freewheeling mode, where the SMES coil is re-turned to PM. The control system uses PS , and S_1 to maintain the state, ensuring minimal energy loss. The governing equation continues to focus on maintaining the balance between the current in the SMES and the voltage across the capacitor.

During the pulse generation phase, the system shifts to using IGBT S_2 while keeping IGBTs PS on to move SMES in PM phase and S_1 in off condition to discharge the capacitor into the pulsed load. The circuit is shown in Fig. 3(c) and the governing equation is provided in (3), which happens at time t_2 . $I_{s,2}$ is the initial current in SMES, and $U_{c,2}$ is voltage in capacitor C at $t = t_2$.

When voltage across the capacitor goes below a certain predefined value the IGBTs PS , turns off and S_1 turns on to charge the capacitor back to the referenced voltage value for the pulse while S_2 is still on and supplying the pulse current to the load. This phase introduces more complex differential equations, accounting for both the inductance of the pulsed load L_m and the resistance R_m . The current in the pulsed load i_m is expressed in (4) and the circuit is shown in Fig. 3(d), which happens at time t_3 . $I_{s,3}$ is the initial current in SMES, $U_{c,3}$ is voltage in capacitor C , and $I_{m,3}$ is the initial current in the pulsed load at $t = t_3$.

Eqs. (3), and (4) together describe how the stored energy in the capacitor is transferred to the pulsed load, generating the desired current pulse.

$$\begin{aligned}
 u_c(t_2) &= U_{c,2} \\
 i_s(t_2) &= I_{s,2} \\
 \frac{di_s}{dt} &= -\frac{R_{on1}}{L_s} \cdot i_s \\
 i_m(t_2) &= 0 \\
 \frac{di_m}{dt} &= \frac{[u_c - (R_{on} + R_m) \cdot i_m]}{L_m} \\
 \frac{du_c}{dt} &= -\frac{i_m}{C} \\
 u_c(t_3) &= U_{c,3} \\
 i_s(t_3) &= I_{s,3} \\
 i_m(t_3) &= I_{m,3} \\
 \frac{di_s}{dt} &= -\frac{(u_c + R_{on} \cdot i_s)}{L_s} \\
 \frac{di_m}{dt} &= \frac{[u_c - (R_{on} + R_m) \cdot i_m]}{L_m} \\
 \frac{du_c}{dt} &= \frac{(i_s - i_m)}{C}
 \end{aligned} \tag{3}$$

$$\begin{aligned}
 \frac{di_s}{dt} &= -\frac{(u_c + R_{on} \cdot i_s)}{L_s} \\
 \frac{di_m}{dt} &= \frac{[u_c - (R_{on} + R_m) \cdot i_m]}{L_m} \\
 \frac{du_c}{dt} &= \frac{(i_s - i_m)}{C}
 \end{aligned} \tag{4}$$

Once the pulse reaches the flat-top phase, the PWM switching of the control system maintains the current at a constant level. The control system continuously monitors the voltage and current in the pulsed load to ensure that the desired pulse shape is maintained. This phase is crucial in pulsed power

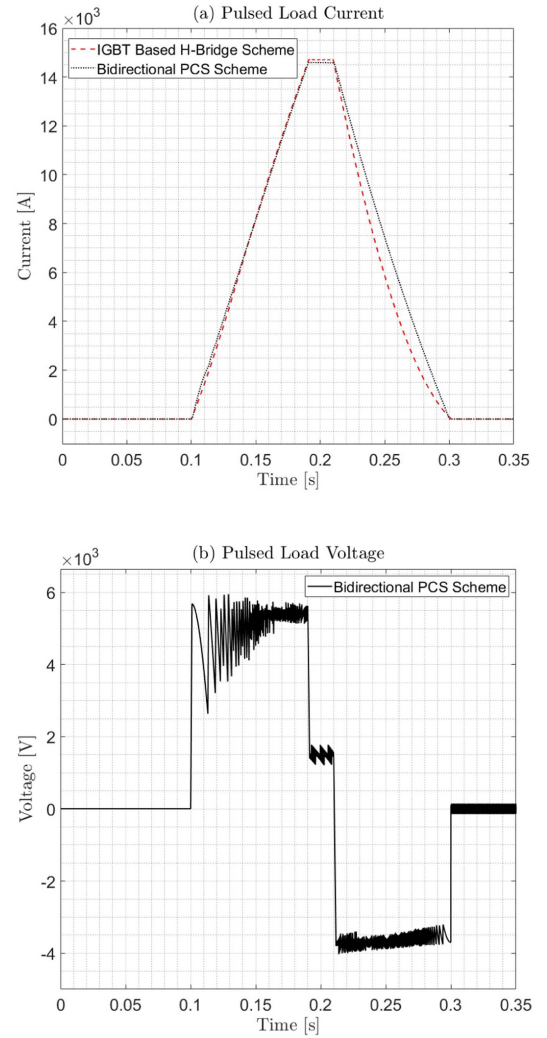


Fig. 4. Bidirectional PCS current (a) and voltage (b).

applications where precise current control is required to meet the specifications of the experiment or process.

The final phase involves the recovery of energy from the pulsed load. The remaining energy is transferred back to the SMES through capacitor C with the control system regulating the process using PWM. The circuit is shown in Fig. 3(e) and (f). The recovery process can be described by Eqs. (2), (3), and (4). These equations govern the behavior of the energy recovery process, ensuring that any excess energy is efficiently stored back into the SMES for future use. The control system adjusts the IGBTs to manage the flow of energy and prevent overcharging or voltage spikes in the capacitors.

IV. RESULTS OF THE SIMULATIONS AND DISCUSSION

To validate the performance of the novel PCS design for SMES, simulations were conducted to analyze efficiency, pulse generation capability, and energy recovery process. The results of the bidirectional DC/DC converter are presented in Fig. 4, providing insights into the operational performance under various conditions.

In the simulation, the current pulses generated by the PCS show that the current is ramped up smoothly, reaching the desired flat-top value before decaying in a controlled manner. The pulsed load current, i_m , is shown in Fig. 4(a), highlighting the effectiveness of the PCS in delivering the required current pulses. The simulation results show that the current in the pulsed load reached approximately 15 kA, with the converter displaying the precision in pulse shaping, especially during the flat-top phase. The corresponding voltage across the terminals of the pulsed load is shown in Fig. 4(b). The converter showed a consistent and controlled voltage profile. This voltage control is crucial for pulsed power applications, where voltage fluctuations can negatively impact the performance of the load.

One of the critical factors evaluated in the simulations was energy recovery. After the pulse generation and delivery phase, the PCS design was tested for its ability to recover and store the remaining energy in the SMES. The bidirectional converter's ability to manage bidirectional power flow allowed efficient energy transfer back to the SMES. Low losses due to the reduced number of converters and the corresponding heat generation in the PCS make it less burden on thermal management. The peak power delivered to the pulsed load reached approximately 80 MW, which without an efficient system will raise the temperature of the components and lower the lifetime of the system. This might introduce the burden on the cryogenics system.

V. CONCLUSION

A design and analysis of a novel PCS topology for SMES in pulsed power applications is reported. The bidirectional DC/DC converter is an innovative approach to improving energy transfer efficiency, pulse shaping, and energy recovery. The converter eliminates the traditional H-bridge architecture, introducing a more streamlined and efficient design that excels in energy delivery and recovery. The simulations showed that the bidirectional converter precisely provides the desired pulse shape. The novel PCS system is scalable and efficient for large power loads such as pulsed magnets.

REFERENCES

- [1] A. Evans, V. Strezov, and T. Evans, "Energy storage technologies," in *Encyclopedia of Energy Storage*, M. A. Abraham, Ed., Amsterdam, The Netherlands: Elsevier, 2024, pp. 548–555, doi: [10.1016/B978-0-323-90386-8.00030-9](https://doi.org/10.1016/B978-0-323-90386-8.00030-9).
- [2] A. K. Panda and T. Pentia, "Design and modeling of SMES based SAPF for pulsed power load demands," *Int. J. Elect. Power Energy Syst.*, vol. 92, pp. 114–124, Nov. 2017, doi: [10.1016/j.ijepes.2017.04.011](https://doi.org/10.1016/j.ijepes.2017.04.011).
- [3] Sonia and A. K. Dahiya, "Superconducting magnetic energy storage coupled static compensator for stability enhancement of the doubly fed induction generator integrated system," *J. Energy Storage*, vol. 44, 2021, Art. no. 103232, doi: [10.1016/j.est.2021.103232](https://doi.org/10.1016/j.est.2021.103232).
- [4] R. Piovan, E. Gaio, F. Lunardon, and A. Maistrello, "MEST: A new magnetic energy storage and transfer system for improving the power handling in fusion experiments," *Fusion Eng. Des.*, vol. 146, pp. 2176–2179, 2019, doi: [10.1016/j.fusengdes.2019.03.146](https://doi.org/10.1016/j.fusengdes.2019.03.146).
- [5] A. Morandi, B. Gholizad, and M. Fabbri, "Design and performance of a 1 MW-5 s high temperature superconductor magnetic energy storage system," *Supercond. Sci. Technol.*, vol. 29, no. 1, 2015, Art. no. 015014, doi: [10.1088/0953-2048/29/1/015014](https://doi.org/10.1088/0953-2048/29/1/015014).
- [6] Q. Sun, H. Lv, S. Gao, K. Wei, and M. Mauersberger, "Optimized control of reversible VSC with stability mechanism study in SMES based V2G system," *IEEE Trans. Appl. Supercond.*, vol. 29, no. 2, Mar. 2019, Art. no. 5401106, doi: [10.1109/TASC.2019.2891822](https://doi.org/10.1109/TASC.2019.2891822).
- [7] J. Glowacki, M. Goddard-Winchester, R. A. Badcock, and N. J. Long, "Superconducting magnetic energy storage for a pulsed plasma thruster," in *Proc. AIAA Propulsion Energy 2020 Forum*, 2020, Art. no. 3635, doi: [10.2514/6.2020-3635](https://doi.org/10.2514/6.2020-3635).
- [8] M. H. Ali, B. Wu, and R. A. Dougal, "An overview of SMES applications in power and energy systems," *IEEE Trans. Sustain. Energy*, vol. 1, no. 1, pp. 38–47, Apr. 2010, doi: [10.1109/TSST.2010.2044901](https://doi.org/10.1109/TSST.2010.2044901).
- [9] J. R. Sims, D. G. Rickel, C. A. Swenson, J. B. Schillig, G. W. Ellis, and C. N. Ammerman, "Assembly, commissioning and operation of the NHMFL 100 tesla multi-pulse magnet system," *IEEE Trans. Appl. Supercond.*, vol. 18, no. 2, pp. 587–591, Jun. 2008, doi: [10.1109/TASC.2008.922541](https://doi.org/10.1109/TASC.2008.922541).
- [10] J. Sims et al., "First 100 T non-destructive magnet," *IEEE Trans. Appl. Supercond.*, vol. 10, no. 1, pp. 510–513, Mar. 2000, doi: [10.1109/77.828284](https://doi.org/10.1109/77.828284).
- [11] J. R. Michel, S. B. Betts, J. D. Lucero, A. Bhardwaj, L. N. Nguyen, and D. N. Nguyen, "Design and construction of the new 85 T duplex magnet at NHMFL-los alamos," *IEEE Trans. Appl. Supercond.*, vol. 34, no. 5, Aug. 2024, Art. no. 4900305, doi: [10.1109/TASC.2023.3338580](https://doi.org/10.1109/TASC.2023.3338580).
- [12] C. Huang, X. Y. Xiao, Z. Zheng, and Y. Wang, "Cooperative control of SFCL and SMES for protecting PMSG-based WTGs under grid faults," *IEEE Trans. Appl. Supercond.*, vol. 29, no. 2, Mar. 2019, Art. no. 5601106, doi: [10.1109/TASC.2019.2891908](https://doi.org/10.1109/TASC.2019.2891908).
- [13] Á. Ortega and F. Milano, "Generalized model of VSC-based energy storage systems for transient stability analysis," *IEEE Trans. Power Syst.*, vol. 31, no. 5, pp. 3369–3380, Sep. 2016, doi: [10.1109/TPWRS.2015.2496217](https://doi.org/10.1109/TPWRS.2015.2496217).
- [14] W. Gil-González, O. D. Montoya, A. Garcés, and G. Espinosa-Pérez, "IDA-passivity-based control for superconducting magnetic energy storage with PWM-CSC," in *Proc. IEEE 9th Annu. IEEE Green Technol. Conf.*, Denver, CO, USA, 2017, pp. 89–95, doi: [10.1109/GreenTech.2017.19](https://doi.org/10.1109/GreenTech.2017.19).
- [15] M. Farahani and S. Ganjefar, "Solving LFC problem in an interconnected power system using superconducting magnetic energy storage," *Physica C, Supercond.*, vol. 487, pp. 60–66, 2013, doi: [10.1016/j.physc.2013.02.005](https://doi.org/10.1016/j.physc.2013.02.005).
- [16] H. F. Latorre, M. Ghandhari, and L. Söder, "Active and reactive power control of a VSC-HVdc," *Electric Power Syst. Res.*, vol. 78, no. 10, pp. 1756–1763, 2008, doi: [10.1016/j.epsr.2008.03.003](https://doi.org/10.1016/j.epsr.2008.03.003).
- [17] A. Bhardwaj et al., "Superconducting magnetic energy storage for pulsed power magnet applications," *IEEE Trans. Appl. Supercond.*, vol. 33, no. 5, Aug. 2023, Art. no. 5700306, doi: [10.1109/TASC.2023.3265620](https://doi.org/10.1109/TASC.2023.3265620).
- [18] A. Bhardwaj, J. Moon, and S. V. Pamidi, "Design of power conversion system for pulsed power applications of SMES," in *Proc. SoutheastCon 2024*, Atlanta, GA, USA, 2024, pp. 1464–1469, doi: [10.1109/Southeast-Con52093.2024.10500098](https://doi.org/10.1109/Southeast-Con52093.2024.10500098).
- [19] A. Bhardwaj et al., "Modeling and measurements of ramping losses in HTS coils for pulsed power applications of SMES," *IEEE Trans. Appl. Supercond.*, vol. 34, no. 3, May 2024, Art. no. 5700407, doi: [10.1109/TASC.2024.3356427](https://doi.org/10.1109/TASC.2024.3356427).
- [20] H. J. Boenig, J. B. Schillig, H. E. Konkel, P. L. Klingner, T. L. Petersen, and J. D. Rogers, "Design installation and commissioning of the los alamos national laboratory pulsed power generator," *IEEE Trans. Energy Convers.*, vol. 7, no. 2, pp. 260–266, Jun. 1992, doi: [10.1109/60.136219](https://doi.org/10.1109/60.136219).
- [21] J. B. Schillig et al., "Design and testing of a 320 MW pulsed power supply," in *Proc. Conf. Rec. 1997 IEEE Ind. Appl. Conf. 32nd IAS Annu. Meeting*, New Orleans, LA, USA, 1997, vol. 2, pp. 1600–1607, doi: [10.1109/IAS.1997.629065](https://doi.org/10.1109/IAS.1997.629065).
- [22] S. S. Kalsi, *Applications of High Temperature Superconductors to Electric Power Equipment*. Hoboken, NJ, USA: Wiley, 2011, pp. 261–303, doi: [10.1002/9780470877890](https://doi.org/10.1002/9780470877890).
- [23] J. M. Maza-Ortega, E. Acha, S. García, and A. Gómez-Expósito, "Overview of power electronics technology and applications in power generation transmission and distribution," *J. Modern Power Syst. Clean Energy*, vol. 5, no. 4, pp. 499–514, 2017, doi: [10.1007/s40565-017-0308-x](https://doi.org/10.1007/s40565-017-0308-x).